THE ASTROPHYSICAL JOURNAL, 313:185–191, 1987 February 1

A 9 MONTH LONG SOFT X-RAY SURVEY OF THE LARGE MAGELLANIC CLOUD. I. X-RAY MAP AT $\frac{1}{4}$ keV

K. P. SINGH,[1] J. A. NOUSEK, D. N. BURROWS, AND G. P. GARMIRE
The Pennsylvania State University
Received 1985 April 22; accepted 1986 July 18

ABSTRACT

We present a $\frac{1}{4}$ keV X-ray map of the Large Magellanic Cloud (LMC) obtained from 9 months of scanning observations with the *HEAO 1* low energy detectors. This soft X-ray map is the most sensitive $\frac{1}{4}$ keV survey of this region yet reported. A detailed comparison of the $\frac{1}{4}$ keV X-ray observations with the neutral hydrogen column densities in the LMC obtained from a new 21 cm line survey shows no evidence for absorption effects is found, which in the $\frac{1}{4}$ keV X-ray flux from the LMC due to the neutral matter in the LMC. Instead, faint X-ray emission invalidates attempts to use the LMC to measure any hypothetical cosmic $\frac{1}{4}$ keV X-ray background, at least for instruments which are unable to spatially resolve the LMC emission.

The extent of the observed emission is smaller than the size of the halo (24°) or the disk (14°) of the LMC. Assuming this $\frac{1}{4}$ keV emission to be diffuse, we identify it with two large regions in the LMC—a supergiant shell of optical nebulosity known as Shapley III and the bar of the LMC. The X-ray luminosities of these two regions are estimated to be 3.4×10^{37} ergs s^{-1} and 7.2×10^{37} ergs s^{-1} (0.1–1.0 keV), respectively. Shapley III could be the first X-ray superbubble observed in an external galaxy.

Subject headings: galaxies: Magellanic Clouds — nebulae: supernova remnants — X-rays: sources

I. INTRODUCTION

The $\frac{1}{4}$ keV X-ray emission from the Large Magellanic Cloud (LMC) has been surveyed only twice over the past decade. These surveys were carried out using sounding rockets, and their results were reported by Rappaport *et al.* (1975) and Long, Agrawal, and Garmire (1976). We report the results of 9 months of scanning observations of the LMC with the *HEAO 1* A2[2] low energy detector (LED) and present the resulting $\frac{1}{4}$ keV X-ray map of the LMC.

Our analysis of the $\frac{1}{4}$ keV X-ray data from the LMC shows a complete lack of modulation of $\frac{1}{4}$ keV X-rays due to absorption by the neutral matter in the LMC. There is no evidence for X-ray emission from either the disk or the halo of the LMC. However, two large emission regions positionally associated with well-known optical features in the LMC are detected in the $\frac{1}{4}$ keV band. These may arise, in part, from diffuse emission produced by hot gas associated with the optical objects. One of these faint X-ray features coincides with a supergiant shell of optical nebulosity known as Shapley III and the other with the LMC bar.

II. OBSERVATIONS

The *HEAO 1* A2 experiment has been described in detail by Rothschild *et al.* (1979). It consists of six multiwire, multilayer gas proportional counters sensitive over the 0.18–60 keV energy range. The X-ray data reported here were taken with the low energy detector (LED 1), which is sensitive in the 0.18–2.8 keV band and has two mechanically collimated fields of view [1°.55 × 2°.95 (FWHM) and 2°.92 × 2°.80 (FWHM)] mounted in a plane perpendicular to the spin axis. The LED 1 data considered here were collected from the narrower field of view of this detector as it scanned the sky while the spin axis was kept pointed toward the Sun. Each satellite rotation (nominal period was 33 minutes) provided a scan of a great circle through the ecliptic poles with a width of 2°.95 (FWHM) on the sky. Different great circles were described as the spin axis was stepped by 0°.5 every 12 hr to keep it pointed at the Sun. Since the LMC is located very close to an ecliptic pole, it was observed on almost every scan between 1977 August 17 and 1978 May 23, when the detector gas supply was depleted and the detector shut down.

The LED 1 proportional counter has four layers of wire grids, a grid cover, a thin polypropylene window, and propane counting gas. Incident X-rays are detected in the top layer (M1) and the middle two layers, which are combined together to form M2. Two other sets of anodes, V1 and V2, form an anticoincidence shield around the M1 and M2 layers and are used to reject charged particles that penetrate the gas volume. In addition, M1 and M2 are in anticoincidence, thereby rejecting charged particles passing through the collimators and reaching the M2 layer. The detection efficiencies of the different layers in LED 1 are shown in Figure A1 of Rothschild *et al.* (1979). Only X-rays which induced pulse height events in the first layer of LED 1 and in the broad pulse height band named Discovery Scaler 5 (DS5) were used in this analysis. Figure 1 shows the response of this band as a function of the energy of the incident X-rays. The DS5 band has greatest response to 0.15–0.28 keV X-rays and will be referred to as the $\frac{1}{4}$ keV band.

Normally the LED detector background after vetoing is very low relative to the flux of X-rays observed from the sky. However, the data can be contaminated by charged particles entering the detector due to the changing geomagnetic environment and by fluorescent and scattered solar X-rays from sunlit Earth. The effects of these sources of background have been minimized in the data presented here. First, the V1 and V2 rates were used to estimate the charged particle counting rate (N_e). Data which were obtained when N_e was greater than 3000/40.96 s (see Figs. 9–10 in Rothschild *et al.* 1979) were rejected. With this restriction only 1% of the

[1] On leave from Tata Institute of Fundamental Research, Bombay, India.
[2] The A2 experiment on *HEAO 1* is a collaborative effort led by E. Boldt of GSFC and G. P. Garmire of PSU, with collaborators at GSFC, Caltech, JPL, and the University of California at Berkeley.

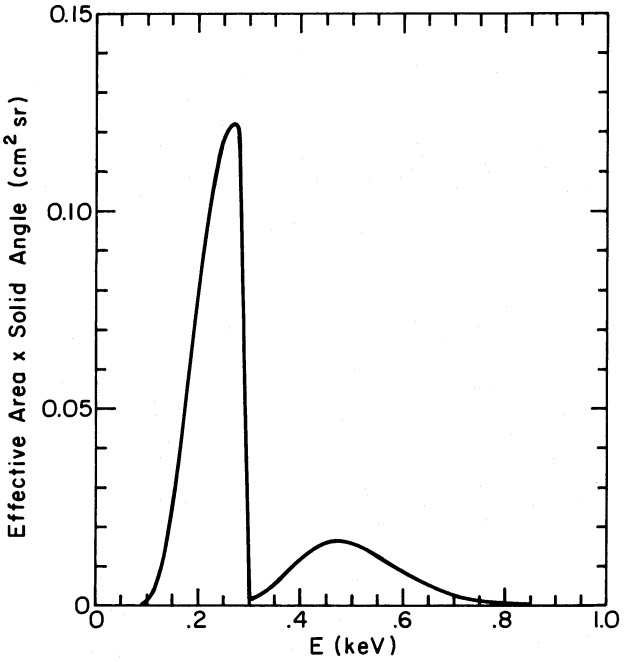

FIG. 1.—The detector response (cm^2 sr) of the low energy detector in the DS5 energy band as a function of the energy of the incident X-rays.

present data corresponds to times when the angle between the magnetic field vector and the detector viewing axis is between 70° and 90° (i.e., when the charged particle flux is the highest). The N_e criterion proved to be better than a magnetic field criterion at excluding contaminated data, so we did not apply a magnetic field restriction directly. Second, to eliminate X-rays scattered from sunlit Earth, data were accepted only when the zenith angle of the observation was less than 90° if the horizon was sunlit (the zenith angle for the horizon was 111°). Since we found that viewing even the dark Earth horizon increases the background, data were collected only when the zenith angle was less than 95° if the horizon was dark. The X-ray data in DS5 were found to be contaminated on many days when the K_p index was very high, where the K_p index is a measure of the solar-related geomagnetic activity which is published regularly in the *Journal of Geophysical Research*.[3] Therefore, the X-ray data in DS5 obtained on days of high K_p index ($K_p > 3$) were rejected. With these exclusions, the X-ray data in this DS5 energy band had a total exposure of 1.29×10^5 s within a $25° \times 25°$ field centered approximately on the LMC (R.A. = 05^h40^m, decl. = $-65°$). After elimination of the contamination described above, we believe that our X-ray data in the region around the LMC are free of systematic or locally produced effects down to a level less than 10% of the $\frac{1}{4}$ keV diffuse sky flux.

In order to facilitate comparison between our X-ray data and the 21 cm data of Rohlfs *et al.* (1984) (Fig. 2*a*), our $\frac{1}{4}$ keV map was produced in the same tangential coordinate system used by Rohlfs *et al.*, centered on the optical center of the bar (R.A. = 05^h24^m, decl. = $-69°47'$) and with pixel size and boundaries matching their N_H map. The data were cast onto this map as follows. The region around the LMC was divided into $0.^\circ2 \times 0.^\circ2$ pixels. For each pixel the total number of counts observed while the center of the field of view was within the pixel was divided by the product of the number of times the center of the field of view fell on the pixel and the sampling time (1.28 s) to create the observed X-ray intensity map. This soft X-ray map (Fig. 2*b*), with a total exposure of 1.25×10^5 s, is the most sensitive $\frac{1}{4}$ keV survey of the LMC region yet reported.

[3] Geomagnetic and Solar Data in *Journal of Geophysical Research* 1977 and 1978.

III. RESULTS AND DISCUSSION

Previous surveys of the diffuse $\frac{1}{4}$ keV background in the vicinity of the LMC (Long, Agrawal, and Garmire 1976; Rappaport *et al.* 1975) have been used to place limits on any $\frac{1}{4}$ keV flux of cosmic origin. The attempts failed to detect any "shadowing" by the LMC and were interpreted as limiting the amount of $\frac{1}{4}$ keV emission originating beyond the LMC. Due to the high statistical precision of our data we were motivated to similarly examine our DS5 map for the possibility of observing faint shadowing induced by the neutral gas in the LMC.

The amount of neutral gas in these directions was measured by the recent 21 cm survey of the LMC by Rohlfs *et al.* (1984). Their map of neutral hydrogen column densities (N_H), ranging from 10^{20} cm^{-2} to 3.5×10^{21} cm^{-2}, is shown in Figure 2*a*. A grayscale map of our $\frac{1}{4}$ keV X-ray intensity is shown in Figure 2*b*, with N_H contours superposed. Some residual contamination in the X-ray data is evident in this map and shows up as isolated high-intensity pixels. The brightest X-ray emission (darkest shading) does come from two regions of low N_H, as expected if shadowing by the LMC is occurring. This inverse correlation does not extend to other low N_H regions, however. (Note the low N_H regions in the northeast, northwest, and southwest corners of Figure 2*b*). We take this as evidence that the X-ray structure is of more complex origin than simple shadowing of an isotropic background component.

For direct comparison with previous studies, we fitted a simple model consisting of an isotropic "local" unabsorbed component plus an isotropic "cosmic" component absorbed by the LMC gas. The LMC absorption was determined by convolving the transmission inferred from the N_H map over the X-ray beam for each pixel of the $\frac{1}{4}$ keV map. We used an effective X-ray absorption cross section of 0.8×10^{-20} cm^2 [determined by folding collisional equilibrium plasma spectra within the range $10^{5.9}$–$10^{6.1}$ K (Raymond and Smith 1977, 1984); and N_H in the range 4–8 $\times 10^{20}$ cm^{-2}; through the DS5 energy response and comparing the results with the unabsorbed case].

The observed DS5 X-ray intensity is plotted against the transmission-weighted effective N_H in Figure 3. If the hypothesis of shadowing were valid this plot should show an anticorrelation, but in fact we see just the opposite trend. The linear correlation coefficient is +0.29 for 1018 degrees of freedom, which has probability of occurring by chance of only 0.005. If the shadowing model is fitted to the data the minimum χ^2 occurs for a "local" component of 4.86 counts s^{-1} and a "cosmic" component of 0.01 counts s^{-1}, but the value of reduced χ^2 for these parameters is 1.96 for 1086 degrees of freedom. Note that the size of the "cosmic" component is in agreement with prior experiments, but the value is also meaningless because the model is resoundingly rejected based on its poor minimum χ^2 value ($P \ll 0.001$). We conclude, then, that these data, and prior work of lower angular resolution and statistical precision, cannot meaningfully constrain the amount of trans-LMC $\frac{1}{4}$ keV emission.

The positive correlation discussed above indicates that the

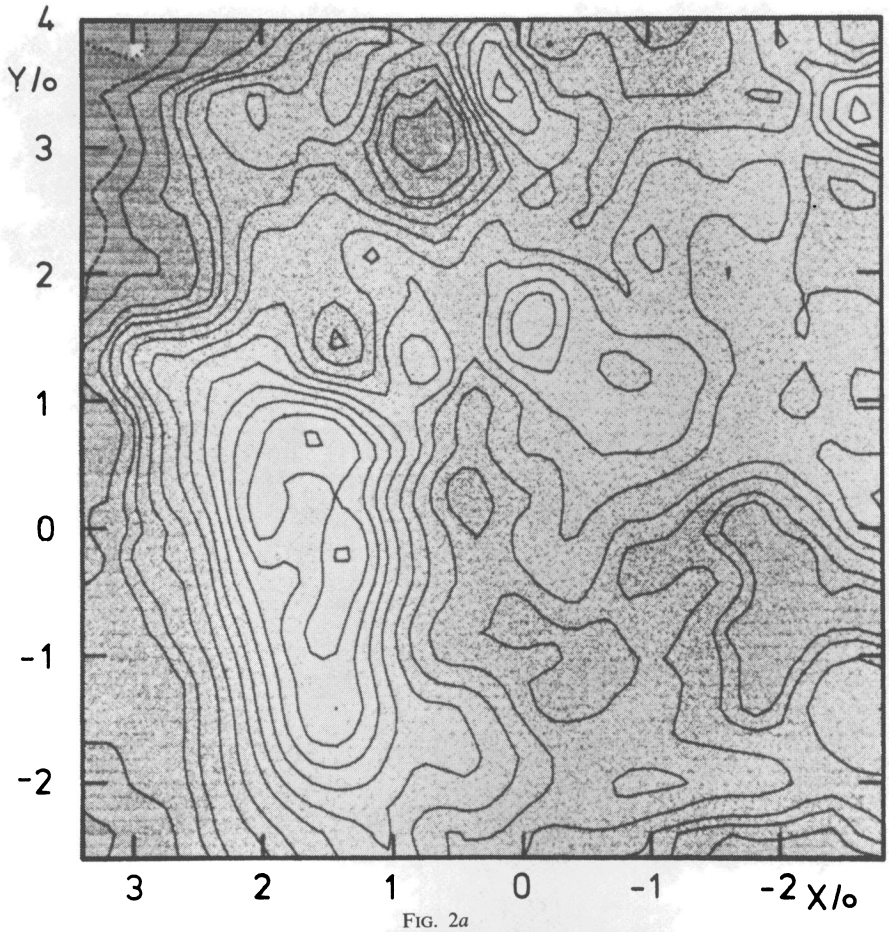

FIG. 2a

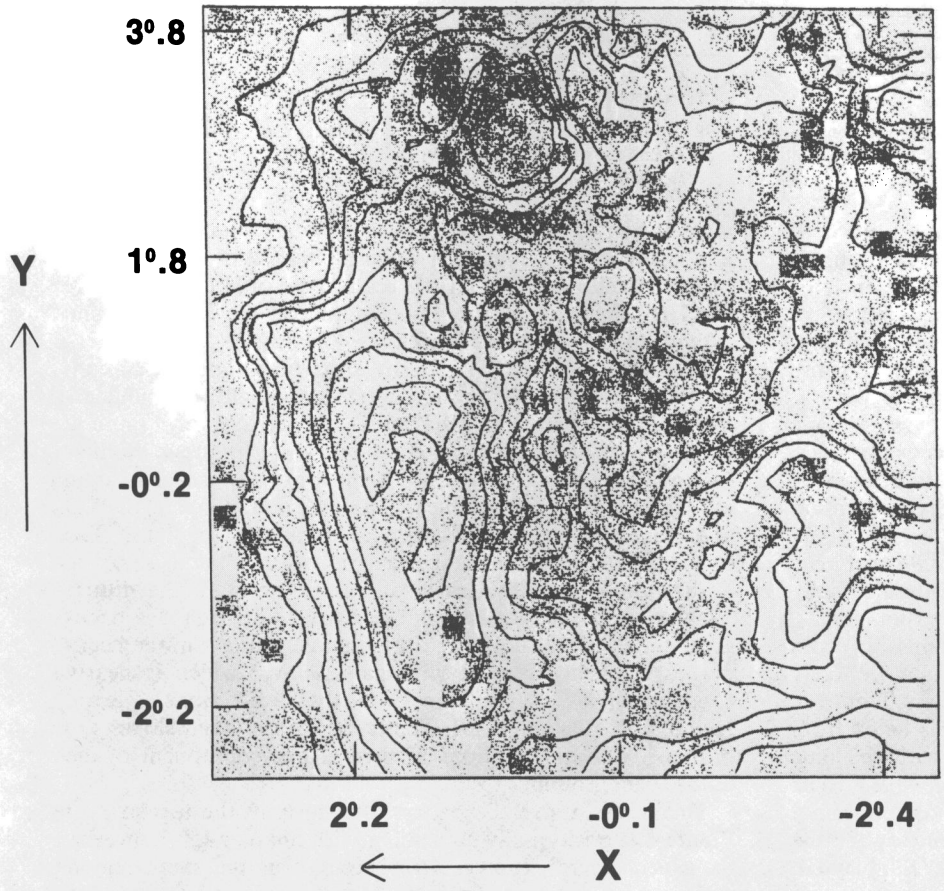

FIG. 2b

FIG. 2a.—The distribution of neutral hydrogen in the LMC reproduced from Rohlfs *et al.* (1984). Contour levels are at equivalent column densities of 0.3×10^{20} atoms cm^{-2}, 0.5×10^{20}, 1, 2, 3, 4, 6, 8, 10, 12, 15, 20, 25, 30, 35×10^{20} atoms cm^{-2}. The shading becomes lighter with increasing surface density.

FIG. 2b.—The *HEAO* A2 LED 1 grayscale map of the LMC in the DS5 (0.18–0.28 keV) energy band superposed on the contour plot of N_H from Fig. 2a. The shading becomes darker as the intensity increases linearly from 4 counts s^{-1} to 12 counts s^{-1}. Contour levels for N_H are at 1, 3, 5, 7, 10, 15, 20, 30×10^{20} atoms cm^{-2}.

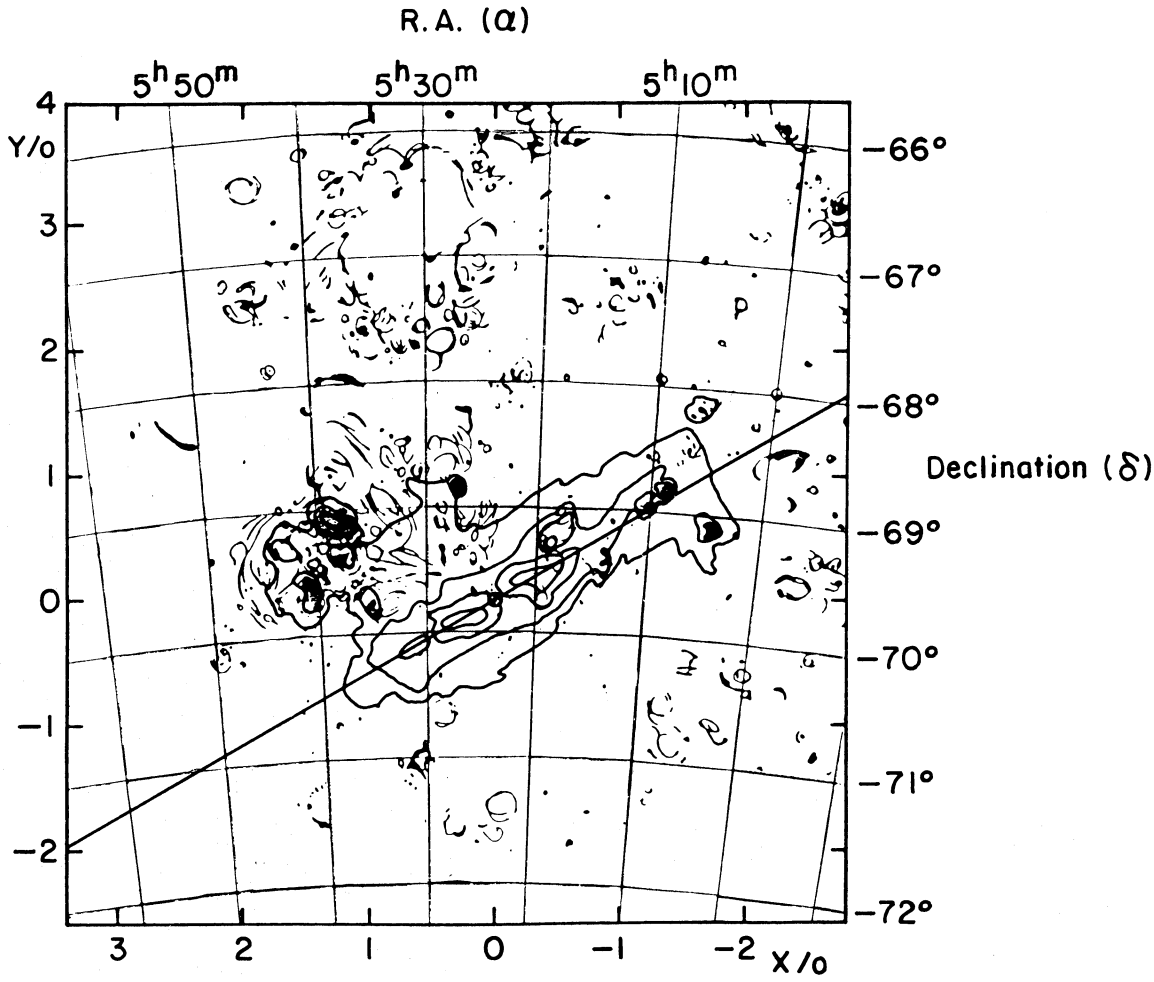

FIG. 2*c*.—The optical image of the Large Magellanic Cloud reproduced from Rohlfs *et al.* (1984). Emission regions from Davies *et al.* are overlaid with blue isophotes of the bar from de Vaucouleurs (1957). The bar is oriented at the position angle 120° and shown as the straight line.

LMC is an X-ray emitter. Although the LMC is known to contain numerous X-ray point sources and extended supernova remnants, we believe that our data provide evidence for diffuse emission from the LMC as well. The faint enhancements seen in Figure 2*b* were not detected in previous surveys of the LMC diffuse emission (Long, Agrawal, and Garmire 1976; Rappaport *et al.* 1975) because of the relatively low statistical precision of the earlier experiments, which were made with sounding rocket experiments with short exposure times. Although both enhancements are coincident with regions of low N_H, we do not believe that they are caused by absorption by the neutral LMC gas. Instead, we attribute them to emission by hot gas in the LMC. The extent of these enhancements is very small compared to the size of the LMC disk or halo, which have respective sizes of 14° and 24° (Westerlund 1971); therefore, it is unlikely that we are observing emission from either the disk or the halo of the LMC. It seems more likely that the $\frac{1}{4}$ keV emission is from smaller scale features. Figure 2*c* shows the distribution of optical emission regions taken from Davies, Elliott, and Meaburn (1976), overlaid with the blue isophotes of the LMC bar from de Vaucouleurs (1957). The straight line at a position angle of 120° shows the orientation of the bar adopted by Rohlfs *et al.* The enhancement toward the top of Figure 2*b* is centered on the "constellation" Shapley III, also known as LMC 4 (Meaburn 1980; Dopita, Mathewson, and Ford 1985), which is a supergiant shell of optical nebulosity coinciding with a large circular void of H I gas in Figure 2*a*. The other enhancement is centered on the LMC bar and extends to the north and south of it.

We averaged the $\frac{1}{4}$ keV data in larger bins to permit a quantitative evaluation of these low surface-brightness enhancements. Four "strip scans" along the X-axis of Figure 2 comprised of these larger bins are shown in Figure 4. (Similar "scans" north of $Y = 4°$ are not shown due to a lack of data and the presence of significant contamination by LMC X-3 and H0539−64). The bin sizes are indicated in the figure. The statistical error bars in these bins are typically 1% or less. The dashed line shows the least squares linear fit to the diffuse background on either side of the LMC. Although this background level is not uniform, the observed changes in the background are uncorrelated with galactic N_H, which is nearly constant at $6–7 \times 10^{20}$ cm^{-2} in these directions (Cleary, Heiles, and Haslam 1979). Therefore the observed slopes are probably due to variations in the galactic component of the diffuse background.

The excess above the background level in the top strip of Figure 4 is positionally coincident with Shapley III. However, there are several known X-ray sources in the same region

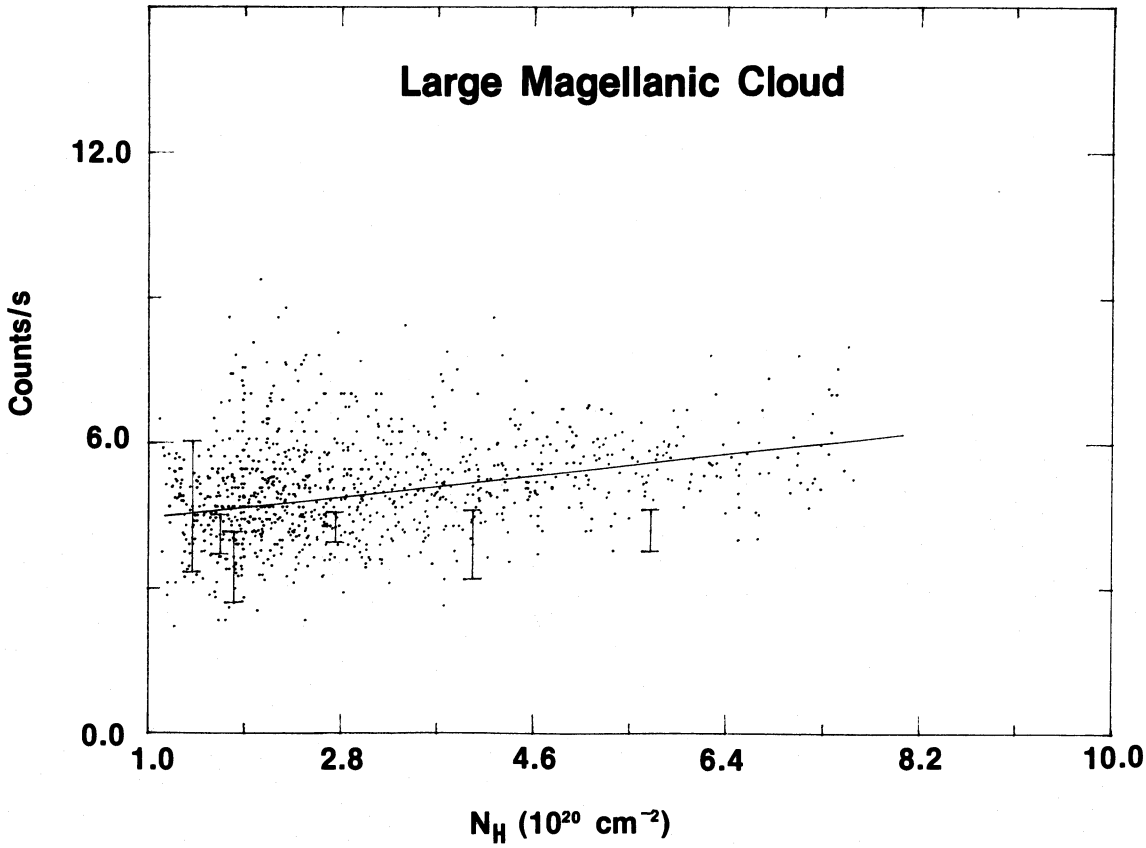

FIG. 3.—The observed X-ray intensity of the LMC in the DS5 (0.18–0.28 keV) energy band versus the effective (weighted with collimator transmission response) column density of H I. The linear fit to the data is shown.

which could be contributing to the DS5 data. As the known sources are in the northern portion of the region, and all would appear pointlike at our resolution, we examined the data in thinner strips to search for the peaked response expected for point sources. The data continue to show a broad response with nearly constant intensity in all strips, but with the widest and strongest enhancement in the southern part of Shapley III. We believe, therefore, that a substantial fraction of the radiation we detect may be coming from the supergiant shell.

The total excess associated with the Shapley III region is equivalent to that produced by a 1.0 counts per second point source. We have estimated the contributions to our data from the brightest supernova remnants near Shapley III: N63 A and N49. Folding the spectral parameters given by Clark *et al.* (1982) through the LED response for the DS5 band gives predicted contributions to our data of 0.21 counts per second and 0.07 counts per second, respectively. Together, these remnants may account for nearly one-third of the excess we found for Shapley III. There are large uncertainties in extrapolating solid state spectrometer (SSS) spectral fits into the DS5 energy band; however we will assume that roughly 0.7 counts per second are due to emission from Shapley III. We believe that the apparently extended enhancement discussed above supports this view. (We note that our measurement of 1.0 counts per second provides an upper bound to the true intensity of emission from Shapley III.)

In order to calculate the physical parameters of the emitting region, we must assume a spectral model. Unfortunately, we cannot constrain the temperature of the $\frac{1}{4}$ keV X-ray enhancements because the emission in our higher energy channels is dominated by the bright LMC sources. We must, therefore, make somewhat arbitrary assumptions about the temperature and column density to use in deriving luminosities and emission measures from our data. The galactic gas toward the LMC gives us a lower limit to the absorbing column density of 6×10^{20} cm^{-2}, and we use this value in our calculations. The temperature can be somewhat constrained by noting that the galactic soft X-ray diffuse background has components with temperatures of 1×10^6 K and 3×10^6 K, and the temperatures of large galactic soft X-ray enhancements tend to be $\sim 2 \times 10^6$ K. Although most diffuse X-ray emission appears to arise under nonequilibrium conditions, our data cannot meaningfully constrain the parameters of nonequilibrium models, so we used the calculations of Raymond and Smith (1977, 1984) for a plasma of solar abundances in thermal equilibrium. This model is most efficient at producing counts in our DS5 band for a temperature of $\sim 2 \times 10^6$ K. We will quote our results assuming a temperature of 2×10^6 K and column density of 6×10^{20} cm^{-2}, since these are reasonable parameters and also provide lower bounds for the emission measure and luminosity required to produce our measured count rates. Under these assumptions, we derive a volume emission measure for Shapley III, $n_e^2 V$, of $1.0 \times 10^{60}(R/0.7)$ cm^{-3}, where R is the count rate in our DS5 band due to emission from the supergiant shell. The corresponding luminosity is 3.4×10^{37} $(R/0.7)$ ergs s^{-1} (0.1–1.0 keV). If a different temperature or a higher column

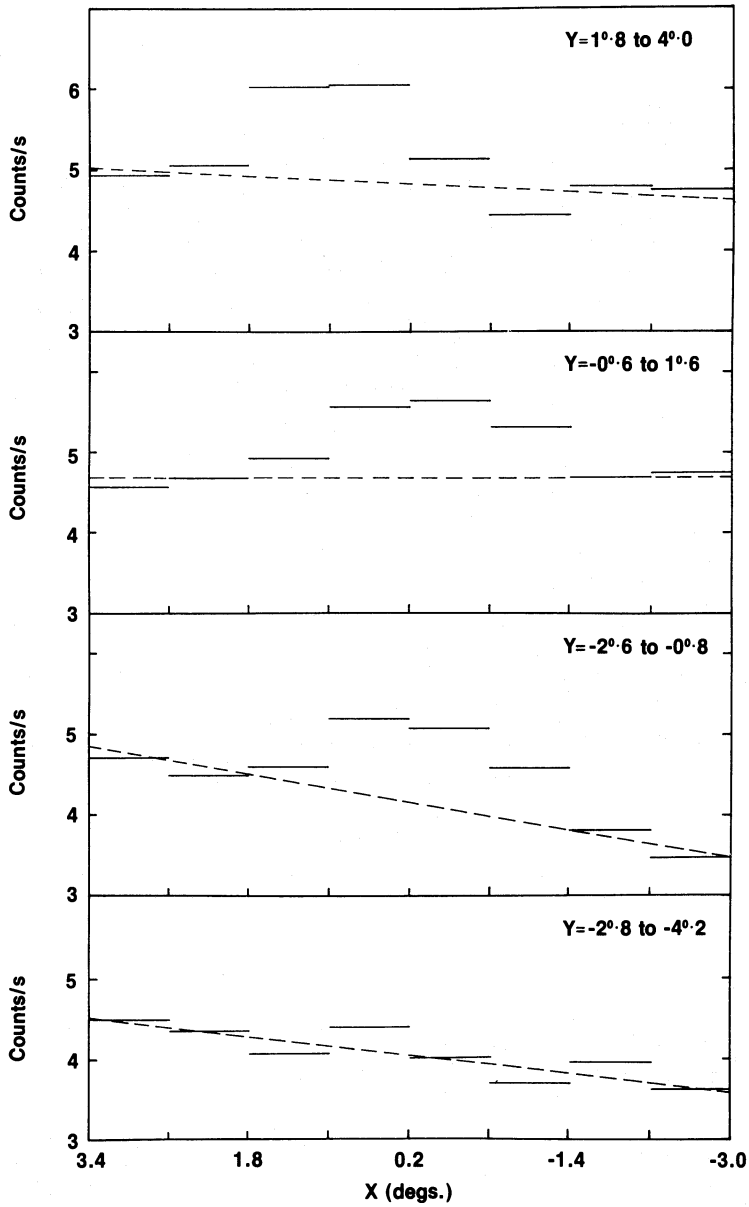

FIG. 4.—The observed X-ray intensity of the LMC in DS5 band summed in four broad regions across the LMC as observed with *HEAO 1* A2. Dashed lines are the least squares fits to the background. The coordinate system is the same as in Fig. 2*a*.

density were assumed, the derived volume emission measure and luminosity would increase (by a factor of 2.5 for a temperature of 1×10^6 K or 4×10^6 K).

Shapley III is a large ring (1400 pc × 1000 pc) outlined by H II regions in the northernmost corner of the LMC (Davies, Elliott, and Meaburn 1976; Meaburn 1980). It encloses a circular void of H I gas (McGee and Milton 1966; Rohlfs *et al.* 1984; Dopita, Mathewson, and Ford 1985) and a large number (~470) of OB stars in numerous associations (Lucke 1974; Braunsfurth and Feitzinger 1983) and is a source of strong far-UV (1250–1600 Å) emission (Page and Carruthers 1978). Emission from 470 OB stars (each with $L_x = 10^{33}$ ergs s^{-1}) falls short of the observed X-ray luminosity of this enhancement by a factor of 70. Therefore, the X-rays are probably truly diffuse in origin. Meaburn (1980) and Feitzinger *et al.* (1981) have shown that this supergiant shell is unlikely to be a wind-driven bubble of an approximately spherical, fossilized supernova remnant produced by a single explosion but is a cylindrical shell punched out of a large H I sheet by the cumulative effects of supernovae and stellar winds from a rapid succession of stellar generations. Assuming a cylindrical shell 1400 pc × 1000 pc across and 200 pc deep (comparable to the scale height of H I in galactic disks), we find an emitting electron density of $0.011(R/0.7)^{1/2}$ cm^{-3} inside the shell. Thus this interpretation implies about $10^{62}(R/0.7)^{1/2}$ H atoms at 2×10^6 K for a total thermal energy content of $7.5 \times 10^{52}(R/0.7)^{1/2}$ ergs. This is comparable to the kinetic energy of the H I shell, which is $\sim 1 \times 10^{53}$ ergs (Dopita *et al.*). This object could be the first extragalactic counterpart of the X-ray superbubble in Cygnus (Cash *et al.* 1980), albeit scaled up by an order of magnitude.

The X-ray enhancement above the background level in the

middle two strips of Figure 4 is positionally coincident with the LMC bar. This excess amounts to 1.9 counts per second, of which a substantial amount is probably due to the numerous point sources and SNRs in the bar. Estimates can be made only of the contributions of the brightest of these sources to our data, since reliable spectra are only available for those. For example, the best-fit parameters for the SSS data for N132 D, N157 B, and 0540−69.3 (Clark *et al.* 1982), when folded through the DS5 response, predict contributions of 0.29, 0.01, and 0.02 counts per second, respectively. The best-fit parameters from an *EXOSAT* observation of N103 B (Singh *et al.* 1987) predict a contribution of 0.07 counts per second to the DS5 data. The other sources are significantly weaker in the *Einstein* IPC than these and probably contribute less to our data, but it is difficult to predict these contributions because of the large difference in the bandpasses of the IPC and our DS5 band. If we assume that approximately 1.5 counts per second arise in a truly diffuse component, then it has a volume emission measure of $n_e^2 V = 2.1 \times 10^{60}(R/1.5)$ cm^{-3} and a luminosity of $7.2 \times 10^{37}(R/1.5)$ ergs s^{-1} (0.1–1.0 keV), assuming the same spectral model we used for Shapley III. (An upper bound to the allowed luminosity is given by setting $R = 1.9$ counts per second.) If the emitting gas fills the LMC bar, it occupies a volume of roughly 2 kpc × 1 kpc × 1 kpc, and the density is $\sim 6 \times 10^{-3}$ cm^{-3}. The thermal energy is then $\sim 3 \times 10^{53}$ ergs.

We note that we cannot establish with certainty a diffuse origin for either of these soft X-ray enhancements. Without better soft X-ray spectral information for the LMC sources, we cannot rule out the possibility that they account for the entire X-ray enhancements that we observe. Furthermore, it is conceivable that a large population of discrete sources with $L_x < 10^{35}$ ergs s^{-1} remains to be discovered in the LMC. Such a population could also produce the enhancements we observe. A more detailed spectral analysis of both bright and faint LMC sources will be required to properly estimate their integrated contribution to the $\frac{1}{4}$ keV band. It is possible, however, that very soft, large, low surface-brightness diffuse emission regions account for these enhancements. A careful analysis of diffuse emission in *Einstein* IPC fields in the vicinity of the LMC might detect these enhancements, if they are truly diffuse.

IV. CONCLUSIONS

The $\frac{1}{4}$ keV X-ray emission observed from the LMC is inconsistent with models of absorption of a cosmic soft X-ray background by the neutral matter in the LMC. In fact, we observe diffuse emission from the LMC, rather than the absorption expected in this model. This result invalidates the technique of using the LMC in an X-ray "shadowing" experiment with coarse angular resolution, as was done by earlier experiments studying diffuse soft X-ray emission from the LMC (Rappaport *et al.* 1975; Long, Agrawal, and Garmire 1976). It is possible that such an experiment can still be performed if the observations have high enough spatial resolution, sensitivity, and statistical precision to resolve the regions of diffuse emission reported here and eliminate them from the study; however, the presence of diffuse emission from the LMC complicates the interpretation of any "shadowing" experiment using the LMC as an absorber.

Two large emission regions in the $\frac{1}{4}$ keV band with very low surface brightness are detected. One of these coincides with a supergiant shell of optical nebulosity known as Shapley III and the other with the LMC bar. If this emission is diffuse with a temperature of $\sim 2 \times 10^6$ K, these regions have luminosities of 3.4×10^{37} and 7.2×10^{37} ergs s^{-1}, respectively (0.1–1.0 keV). Although the physical parameters derived for these regions are highly model-dependent, they indicate scaled-up versions of the X-ray superbubble in Cygnus. Experiments with higher spatial resolution and higher sensitivity in the $\frac{1}{4}$ keV band are required to confirm the identification of these faint features. We do not observe any X-ray emission which could be attributed to the halo of the LMC.

We are extremely thankful to G. M. Weaver for his great interest in the project and for helping us with the data reduction. We thank Professor K. Rohlfs for making the data from his new 21 cm line survey of LMC available to us. It is a pleasure to thank Dr. C. J. Lonsdale for helping in the use of AIPS to produce the maps presented in this paper. One of us (K. P. S.) acknowledges the interesting discussions on this paper with Dr. E. D. Feigelson. We acknowledge the support of NASA under the contract NAS 5-26809.

REFERENCES

Braunsfurth, E., and Feitzinger, J. V. 1983, *Astr. Ap.*, **127**, 113.
Cash, N., Charles, P., Bowyer, S., Walter, F., Garmire, G., and Riegler, G. 1980, *Ap. J. (Letters)*, **238**, L71.
Clark, D. H., Tuohy, I. R., Long, K. S., Szymkowiak, A. E., Dopita, M. A., Mathewson, D. S., and Culhane, J. L. 1982, *Ap. J.*, **255**, 440.
Cleary, M. N., Heiles, C., and Haslam, C. G. T. 1979, *Astr. Ap. Suppl.*, **36**, 95.
Davies, R. D., Elliott, K. H., and Meaburn, J. 1976, *Mem. Roy. Astr. Soc.*, **81**, 89.
de Vaucouleurs, G. 1957, *A.J.*, **62**, 69.
Dopita, M. A., Mathewson, D. S., and Ford, V. L. 1985, *Ap. J.*, **297**, 599.
Feitzinger, J. V., Glassgold, A. E., Gerola, H., and Seiden, P. E. 1981, *Astr. Ap.*, **98**, 371.
Long, K. S., Agrawal, P. C., and Garmire, G. P. 1976, *Ap. J.*, **206**, 411.
Lucke, P. B. 1974, *Ap. J. Suppl.*, **28**, 73.
McGee, R. X., and Milton, J. A. 1966, *Australian J. Phys.*, **19**, 343.
Meaburn, J. 1980, *M.N.R.A.S.*, **192**, 365.
Page, T., and Carruthers, G. R. 1978, *S201 UV Atlas of the Large Magellanic Cloud*, NRL Report 8206 (Washington, D.C.: NRL).
Rappaport, S., Levine, A., Doxsey, R., and Bradt, H. V. 1975, *Ap. J. (Letters)*, **196**, L15.
Raymond, J. C., and Smith, B. W. 1977, *Ap. J. Suppl.*, **35**, 419.
———. 1984, private communication (update to Raymond and Smith 1977).
Rohlfs, K., Kreitschmann, J., Siegman, B. C., and Feitzinger, J. V. 1984, *Astr. Ap.*, **137**, 343.
Rothschild, R. E., *et al.* 1979 *Space Sci. Instr.*, **4**, 269.
Singh, K. P., Westergaard, N. J., Schnopper, H. W., and Helfand, D. J. 1987, in preparation.
Westerlund, B. E. 1971, in *The Magellanic Clouds*, ed. A. B. Muller (Dordrecht: Reidel), p. 31.

D. N. Burrows, G. P. Garmire and J. A. Nousek: Department of Astronomy, 525 Davey Laboratory, The Pennsylvania State University, University Park, PA 16802

K. P. Singh: Danish Space Research Institute, Lundtoftevej 7, 2800 Lyngby, Denmark